

DNA AFFINITY CLEAVING

SEQUENCE SPECIFIC CLEAVAGE OF DNA BY DISTAMYCIN-EDTA · Fe(II) AND EDTA-DISTAMYCIN · Fe(II)

JOHN S. TAYLOR,¹ PETER G. SCHULTZ² and PETER B. DERVAN^{*3}

Division of Chemistry and Chemical Engineering, Contribution Number 6752, California Institute of Technology, Pasadena, CA 91125, U.S.A.

(Received in U.S.A. October 1982)

Abstract—The attachment of EDTA · Fe(II) to distamycin changes the sequence specific DNA binding antibiotic into a sequence specific DNA cleaving molecule. We report the synthesis of EDTA-distamycin (ED) which has the metal chelator, EDTA, tethered to the carboxy terminus of the N-methylpyrrole tripeptide moiety of the antibiotic, distamycin. EDTA-distamycin · Fe(II) (ED · Fe(II)) at 10^{-6} M concentration efficiently cleaves pBR322 DNA (10^{-3} M in base pairs) in the presence of oxygen and dithiothreitol (DTT). Using Maxam-Gilbert sequencing gel analyses, we find that ED · Fe(II) affords DNA cleavage patterns of unequal intensity covering two to four contiguous base pairs adjacent to a five base pair site consisting of adenines (A) and thymines (T). The multiple cleavages at each site might be evidence for a diffusible oxidizing species, perhaps hydroxyl radical. The unequal intensity of cleavage on each side of the A + T site permit assignment of major and minor orientations of the tripeptide binding unit. A comparison of the cleavage specificity of ED · Fe(II) with distamycin-EDTA · Fe(II), (DE · Fe(II)) which has EDTA · Fe(II) attached to the amino terminus of the N-methylpyrrole tripeptide, shows DNA cleavage patterns at the same sites but with intensities of opposite polarity. Maxam-Gilbert sequencing gel analysis of the DNA cleavage patterns by ED · Fe(II) and DE · Fe(II) on both DNA strands of a 381 base pair restriction fragment reveals asymmetric DNA cleavage patterns. Cleavage is shifted to the 3' side of each DNA strand. A model consistent with this cleavage pattern indicates one preferred binding site for ED · Fe(II) and DE · Fe(II) is 3'-TTTAA-5' with the "amino end" of the tripeptide oriented to the 3' end of the thymine rich strand.

This "DNA affinity cleavage" method which consists of attaching cleaving functions to DNA binding molecules followed by DNA cleavage pattern analyses using Maxam-Gilbert sequencing gels may be a useful *direct* method for determining the binding site and orientation of small molecules on native DNA.

Many small molecules important in antibiotic, antiviral, and antitumor chemotherapy bind to double helical DNA. Our knowledge of the base sequence preferences of most DNA binding drugs is somewhat limited due to the restricted information obtained by spectrophotometric analyses of the overall binding affinity on synthetic homopolymer and copolymer DNAs. A smaller class of DNA binding molecules are bifunctional in nature, combining a chemically reactive moiety with a DNA binding unit. One such molecule is the naturally occurring antitumor, antibiotic bleomycin which cleaves DNA in a reaction that depends on Fe(II) and oxygen.⁴ The DNA cleaving function of bleomycin in combination with Maxam-Gilbert sequencing gel analyses affords precise information on the sequence specificity of bleomycin binding. From DNA cleavage patterns obtained from reaction of bleomycin · Fe(II) with end labeled DNA restriction fragments it is known that bleomycin cleaves DNA at the pyrimidine of a two base pair 5'-GT-3' or 5'-GC-3' recognition site.⁵ The structure of the bleomycin · Fe(II):DNA complex is not yet known.⁵

Recently, we synthesized methidiumpropyl-EDTA (MPE), which has the metal chelator, EDTA, tethered to the DNA intercalator, methidium.⁶ MPE · Fe(II) cleaves double helical DNA in the presence of oxygen and reducing agents such as dithiothreitol (DTT) at efficiencies comparable to bleomycin · Fe(II)/DTT. Unlike bleomycin · Fe(II),

MPE · Fe(II) cleaves DNA in a *non-sequence specific* manner consistent with spectrophotometric binding studies that indicate that methidium has no overall base composition specificity.⁷ Because MPE · Fe(II) cleaves DNA with low sequence specificity, partial cleavage of drug protected DNA restriction fragments in combination with Maxam-Gilbert sequencing gel analysis of the DNA cleavage patterns provides a *direct* method, "MPE · Fe(II) footprinting", for determining the locations and size of the binding sites of small molecules on native DNA.⁸

With the discovery that attachment of EDTA · Fe(II) to a DNA binding molecule such as methidium creates an *efficient* DNA cleaving molecule, we undertook the attachment of EDTA to sequence specific DNA binding molecules. The antibiotic distamycin is a tripeptide containing three N-methylpyrrole carboxamides which binds in the minor groove of double helical DNA with a strong preference for adenine and thymine rich regions.⁹ The sequence specificity of distamycin binding presumably results from hydrogen bonding between the amide NHs of the antibiotic and the O(2) of thymines and N(3) of adenines.¹⁰ The N-methylpyrrole tripeptide was chosen as the sequence specific DNA binding unit for the subsequent attachment of EDTA. The EDTA moiety was tethered to the amino terminus of the tripeptide to afford distamycin-EDTA (DE).¹²

In preliminary studies we found that DE · Fe(II) in the presence of O₂ and DTT cleaves DNA, although

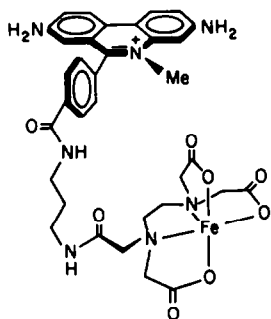


Fig. 1. MPE · Fe(II).

the cleavage is less efficient than with MPE · Fe(II) or bleomycin · Fe(II).¹² Importantly, DE · Fe(II) cleaves DNA restriction fragments at highly localized sites fewer in number than bleomycin · Fe(II).¹² The fewer number of cleavage sites can be explained by larger binding site size requirements for DE · Fe(II) compared to those of bleomycin · Fe(II) whose binding site is known to be two base pairs. Initial studies revealed that DE · Fe(II) caused several DNA strand scissions of unequal intensity clustered on each side of a binding region composed of four A + T bases.¹²

In this manuscript we describe the synthesis and study of EDTA-distamycin (ED), which has the EDTA attached to the carboxy terminus of the tripeptide unit. A comparison of the DNA cleavage patterns produced by DE · Fe(II) and ED · Fe(II) on several restriction fragments affords new information on the binding sites and the preferred orientation of the tripeptide unit, and by extension, distamycin on DNA. Thus the EDTA attachment strategy leads to a class of "DNA affinity cleaving molecules" which allow the binding sites and binding site sizes of small molecules on heterogeneous DNA to be determined *directly*. The synthetic methodology used for the construction of DE and ED should be useful for future work on sequence specific DNA cleaving molecules.

RESULTS

Synthesis of distamycin-EDTA. The N-hydroxy-benzotriazole ester¹³ of the known nitro acid 5,¹⁴ available in eight steps by known methodology from N-methyl-pyrrole-2-carboxylic acid, was condensed with 3-dimethylaminopropylamine to afford nitro amine 6. Subsequent reduction of the nitro group (hydrogen over 5% Pd/C, DMF) afforded diamine 7. This was condensed with the imidazolide¹⁵ of the triethyl ester 10, available in four steps from EDTA. Hydrolysis (0.5M aq LiOH) and acidification gave 3. DE (3) was chromatographed on silica gel (230–400 mesh) with ammonia/ethanol, and was further purified by supporting it on an Amberlite XAD-2 column and washing with 5% aqueous disodium EDTA, distilled water and eluting with methanol (Fig. 3).

Synthesis of EDTA-distamycin. The imidazolide¹⁵ of the nitro acid 5¹⁴ was condensed with excess 3,3'-diamino-N-methyldipropylamine to afford nitro amine 12. This was condensed with the imidazolide of the triethyl ester 9, available in two steps from EDTA, affording the nitro triester 13. Reduction (hydrogen over 5% Pd/C, DMF) of the nitro group, acetylation, hydrolysis of the resulting triester (0.5M aq LiOH) and acidification gave 4. ED (4) was purified by chromatography on silica gel (230–400 mesh) with ammonia/methanol (Fig. 4).

DNA cleavage efficiency. DNA cleavage by DE · Fe(II) and ED · Fe(II) was followed by monitoring the conversion of supercoiled (form I) pBR322 plasmid DNA (10⁻⁵M in base pairs) to open circular and linear forms (forms II and III, respectively).¹⁶ The introduction of one single strand break converts form I to form II. We find that at 10⁻⁶ M concentrations DE · Fe(II) and ED · Fe(II) in the presence of O₂ and DTT cleave DNA, although the cleavage is less efficient than with MPE · Fe(II) or bleomycin · Fe(II) (Table 1).

Sequence specific cleavage. The sequence specific cleavage of heterogeneous double helical DNA by DE · Fe(II) and ED · Fe(II) in the presence of DTT

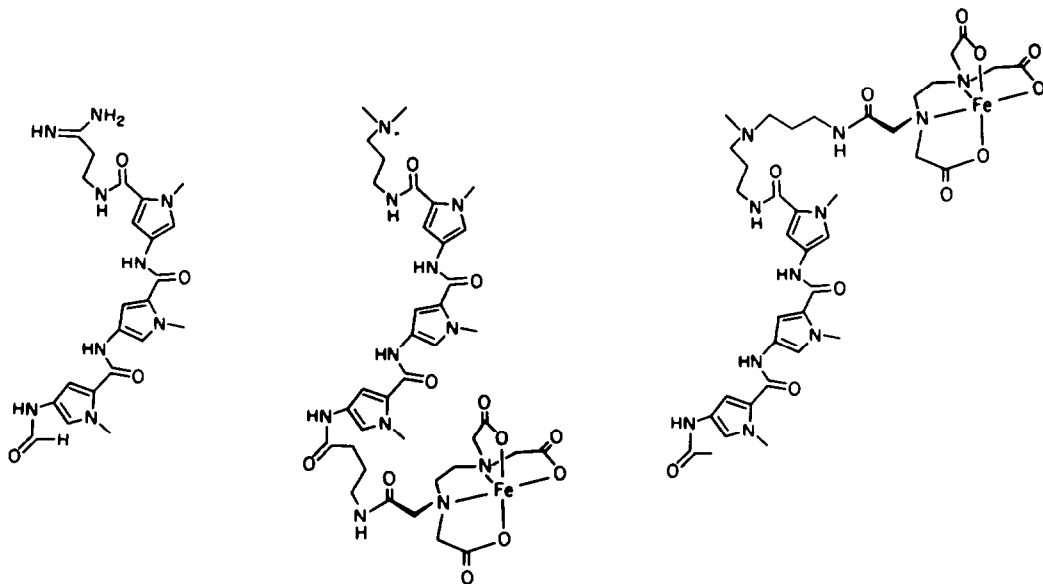


Fig. 2. Left to right: Distamycin A, DE · Fe(II) and ED · Fe(II).

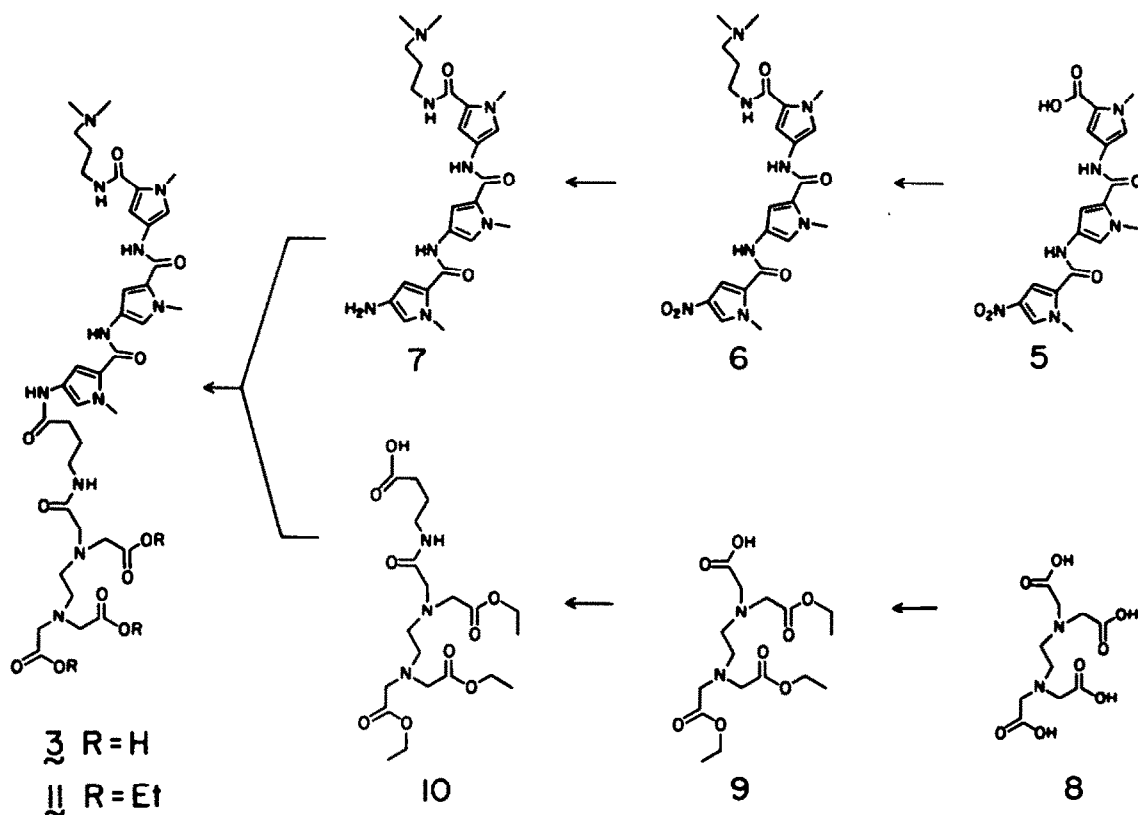


Fig. 3. Synthetic Scheme for DE.

and O_2 was examined on three DNA restriction fragments. These fragments (167, 279, and 381 base pairs in length) were prepared by the usual methods from bacterial plasmid pBR322 DNA and were 3' end labeled with ^{32}P .^{17,18} Each DNA cleaving reagent was allowed to react at two different concentrations with each DNA restriction fragment for 30 min at 25°. The samples were frozen, lyophilized, suspended in formamide, and electrophoresed on a 0.4 mm, 8% polyacrylamide/50% urea Maxam-Gilbert sequencing gel capable of resolving DNA fragments differing in length by one nucleotide.¹⁷ The autoradiogram of the Maxam-Gilbert gel is shown in Fig. 5. The MPE·Fe(II) lanes show a uniform DNA cleavage pattern indicative of relatively non-sequence specific cleavage. In contrast, DE·Fe(II) and

ED·Fe(II) both show a nonrandom pattern with DNA cleavage confined to highly localized sites. A comparison with the Maxam-Gilbert G-lane reveals the A+T rich sites cleaved by DE·Fe(II) and ED·Fe(II). Importantly, the cleavage patterns of DE·Fe(II) and ED·Fe(II) occur in similar locations but with opposite intensity (Fig. 6).

167 Restriction fragment. The 70 bases analyzed from the autoradiogram of the Maxam-Gilbert gel (Fig. 6) for the 167 base pair restriction fragment show two cleavage sites by DE·Fe(II) and three by ED·Fe(II) (12.5 μM concentration, 0.125 DE or ED/base pairs). These cleavage sites cover 2-5 contiguous base pairs separated by the sequence 3'-TTT-5' (base pairs 91-93). The cleavage sites flanking this sequence are of unequal intensity. The

Table 1. Cleavage of pBR322-plasmid in the presence of DTT

Reagent	conc, M	% Form		
		I	II	III
EDTA·Fe(II)	10^{-6}	93	7	0
DE·Fe(II)	10^{-6}	30	70	0
ED·Fe(II)	10^{-6}	4	92	4
MPE·Fe(II)	10^{-7}	0	91	9
Bleomycin·Fe(II)	10^{-7}	0	48	52

Form I pBR322 (10^{-5} M bp), DNA cleaving reagent, buffer (10 mM Tris HCl, 50 mM NaCl, pH 7.4) and DTT (1 mM) were allowed to react at 25°C for 30 minutes and quenched. In all cases reactions were carried to completion. Forms I, II and III were analyzed by agarose gel electrophoresis and quantitated by densitometry after ethidium bromide staining.

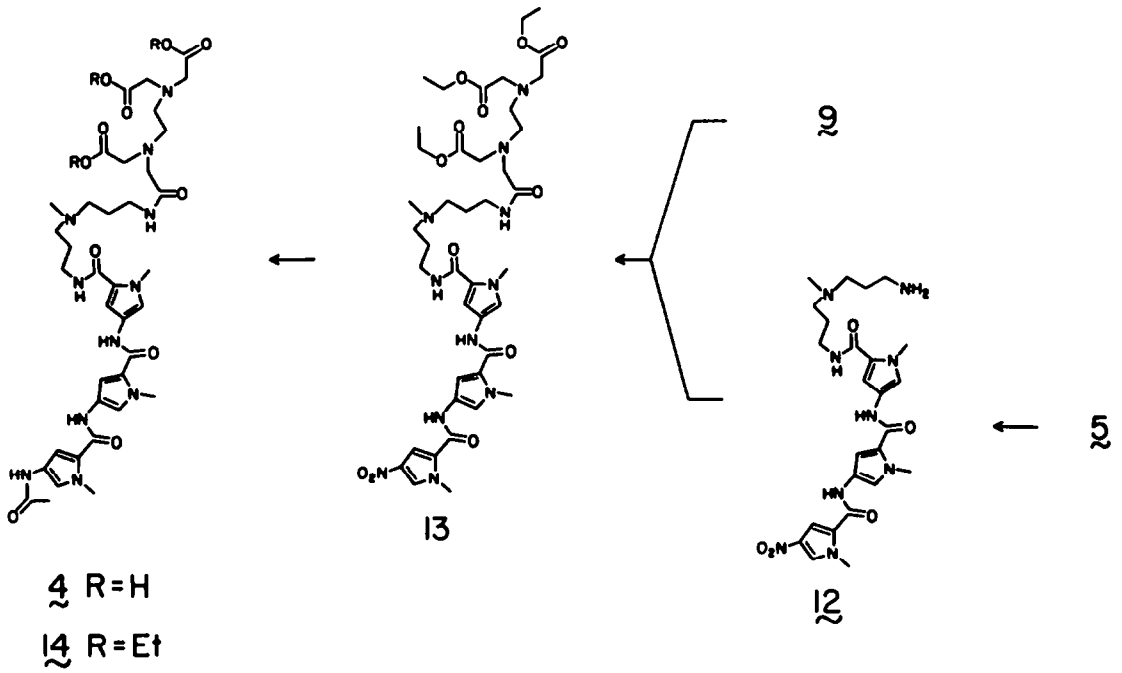


Fig. 4. Synthetic Scheme for ED.

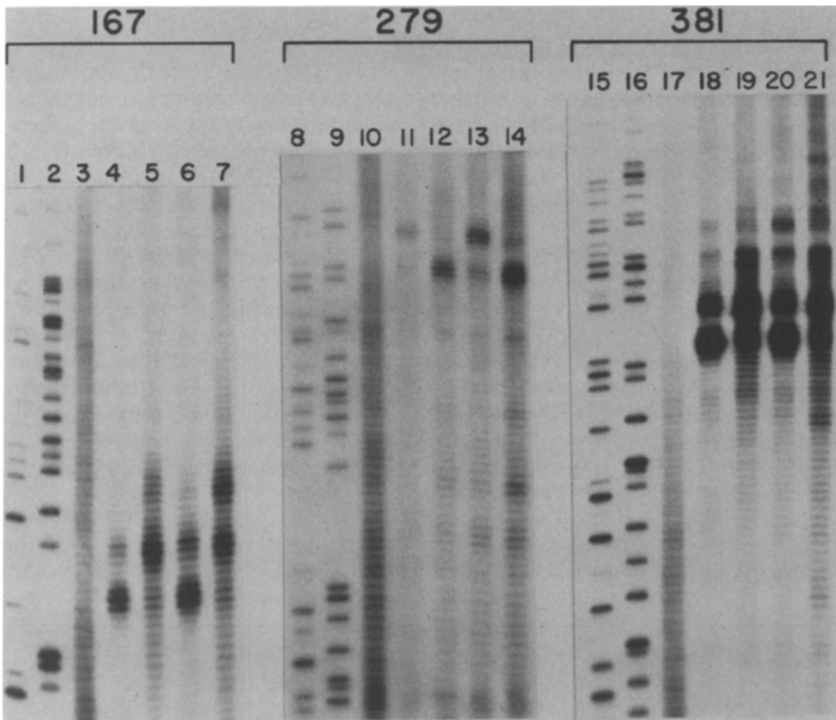


Fig. 5. Autoradiogram of Maxam-Gilbert sequencing gels. Lanes 1, 8, 15: Bleomycin · Fe(II) 4×10^{-6} M; Lanes 2, 9, 16: Maxam-Gilbert G reaction; Lanes 3, 10, 17: MPE · Fe(II) 1×10^{-5} M; Lanes 4, 11, 18: DE · Fe(II) 1.25×10^{-5} M; Lanes 5, 12, 19: ED · Fe(II) 1.25×10^{-5} M; Lanes 6, 13, 20: DE · Fe(II) 5×10^{-5} M; Lanes 7, 14, 21: ED · Fe(II) 5×10^{-5} M. All reactions are made up to 10^{-4} M bp DNA with sonicated calf thymus DNA in 10 mM Tris · HCl, pH 7.8, 50 mM NaCl, 1 mM DTT. Base pairs shown from bottom to top: 77-146 (167 fragment) 68-146 (279 fragment) 77-176 (381 fragment).

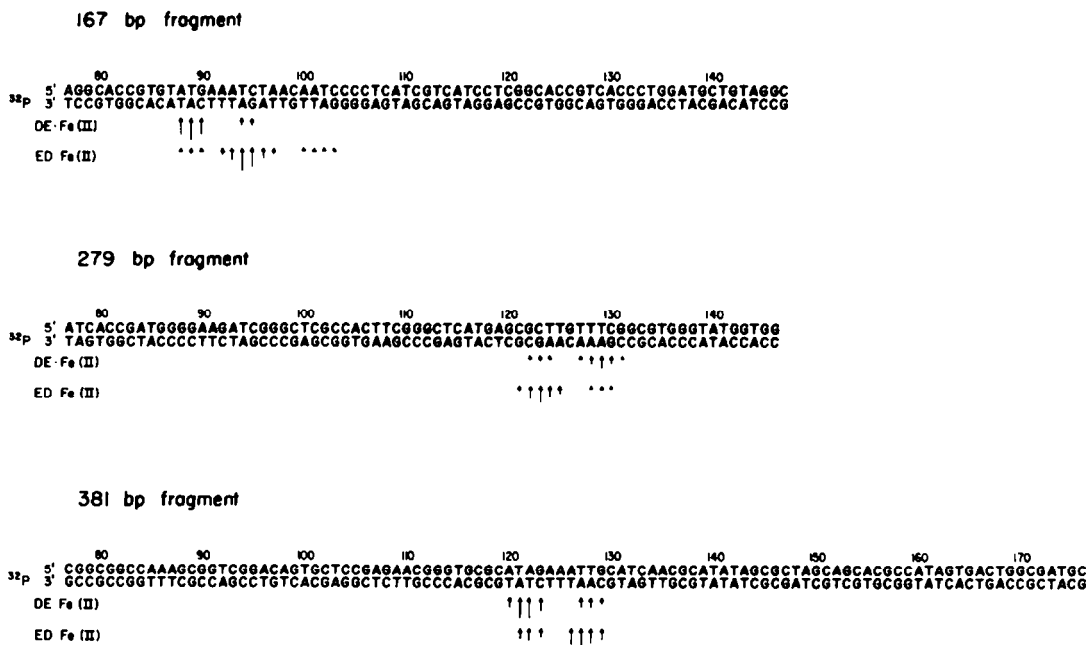


Fig. 6. Histogram of the autoradiogram of the Maxam–Gilbert gels from Fig. 5. Shown are DNA fragments 167 bp, lanes 4 and 5; 279 bp, lanes 11 and 12; and 381 bp, lanes 18 and 19.

major cleavage site for DE·Fe(II) is on the 3' end of the 3'-TTT-5' sequence. The major cleavage site for ED·Fe(II) is on the 5' end.

279 Restriction fragment. The 70 base pairs analyzed from the autoradiogram of the Maxam–Gilbert gel (Fig. 6) for the 279 base pair restriction fragment show two cleavage sites by DE·Fe(II) and ED·Fe(II). The cleavage sites covering 3–5 base pairs are of unequal intensity and flank the sequence 3'-ACA-5' (base pairs 125–127). For DE·Fe(II) the major cleavage is on the 5' end of the 3'-ACA-5' sequence and for ED·Fe(II) it is on the 3' end.

381 Restriction fragment. The 100 bases analyzed from the autoradiogram of the Maxam–Gilbert gel (Fig. 6) for the 381 base pair restriction fragment show two cleavage sites by both DE·Fe(II) and ED·Fe(II). The cleavage sites covering 3–5 base pairs are of unequal intensity and flank the sequence 3'-TTT-5' (base pairs 124–126). For DE·Fe(II), the major cleavage site is on the 3' end of the 3'-TTT-5' sequence and for ED·Fe(II) it is on the 5' end.

Opposite strand analysis. The 381 base pair fragment was labeled at the 5' end of the Bam HI restriction site. The cleavage patterns for DE·Fe(II) and ED·Fe(II) on this 5' end labeled 381 fragment were compared to the cleavage patterns produced on the 3' end labeled strand. The autoradiogram of the gel is shown in Fig. 7. The 70 bases analyzed from the autoradiogram of the Maxam–Gilbert gel (Fig. 7) for the 5' end labeled restriction fragment show a DNA cleavage pattern that is asymmetric, shifted to the 3' end for both DE·Fe(II) and ED·Fe(II) (Fig. 8).

DISCUSSION

Cleavage efficiency. The decreasing order of efficiency for cleavage of supercoiled DNA is bleomycin·Fe(II) > MPE·Fe(II) > ED·Fe(II) >

DE·Fe(II) (Table 1). DE·Fe(II) and ED·Fe(II) cleave DNA at least an order of magnitude less effectively than MPE·Fe(II) or bleomycin·Fe(II). The reduced cleavage efficiency of DE and ED may result from binding constants lower than MPE or bleomycin and/or fewer available binding sites due to higher sequence recognition requirements. MPE·Fe(II) affords a uniform cleavage pattern⁹ and thus can cleave at each of 4362 base pairs of supercoiled pBR322 DNA. DE·Fe(II) and ED·Fe(II) appear to have a five base pair recognition site composed of A + T bases. This could reduce the number of available sites on pBR322 for DE·Fe(II) and ED·Fe(II) cleavage by at least an order of magnitude. Bleomycin·Fe(II) binds guanine-pyrimidines, a two base pair requirement and thus has lower sequence requirements than DE or ED. However, the natural product is probably a more efficient cleaving agent, thereby affording slightly higher cleavage efficiencies than even MPE.

Sequence specificity. The cleavage patterns of DE·Fe(II) and ED·Fe(II) are characterized by two intense cleavage sites covering two to four base pairs separated by a minimum of three A + T base pairs. We believe that DE·Fe(II) and ED·Fe(II) bind to a sequence between the two sites and cleave the flanking bases. The three to five DNA strand scissions on each side of the DE·Fe(II) binding site could reflect the reach of the flexible tether connecting EDTA·Fe(II) to the pyrrole tripeptide, multiple binding modes such as sliding one or two base pairs within that site, or more likely generation of a diffusible reactive species such as hydroxyl radical. The fact that there is a cluster of strand scissions on both sides of the intervening three to four base pair binding sequence suggests that the pyrrole tripeptide groove binder can assume two orientations. The

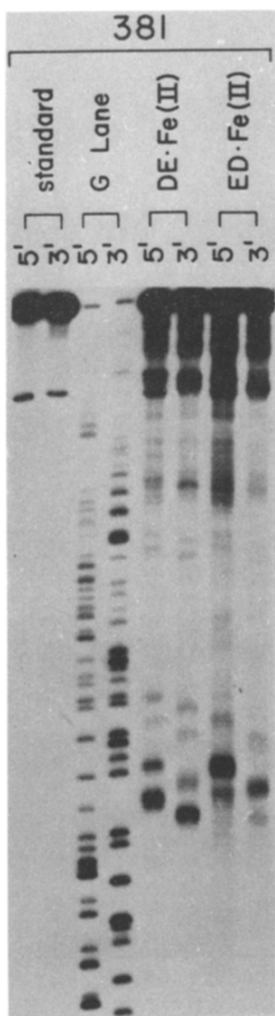


Fig. 7. Autoradiogram of Maxam-Gilbert sequencing gels. $DE \cdot Fe(II)$ $1.25 \times 10^{-5} M$; $ED \cdot Fe(II)$ $1.25 \times 10^{-5} M$. All reactions are made up to $10^{-4} M$ by DNA with sonicated calf thymus DNA in 10 mM. tris \cdot HCl, pH 7.8, 50 mM NaCl, 1 mM DTT.

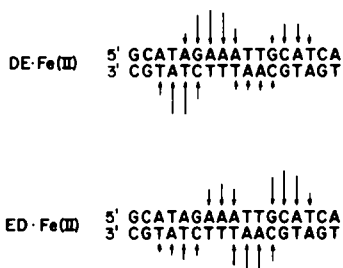


Fig. 8. Histogram of the DNA cleavage patterns on opposite strands taken from the Maxam-Gilbert gel (Fig. 7) of the 381 base pair restriction fragment.

unequal intensity of the cleavage sites reveals the preferred orientation of the tripeptide unit. The opposite polarity of the major cleavage site by DE and ED confirm this interpretation.

The precise correspondence between the cleavage sites and the tripeptide binding site is uncertain from

the single strand analysis. In order to understand the precise relationship between the DNA cleavage patterns and the major and minor binding sites we examined the cleavage patterns on opposite strands of the DNA. The DNA cleavage patterns are asymmetric and shifted to the 3' end. This shift can be understood by examining a model of right-handed B DNA (Fig. 9).

For an $EDTA \cdot Fe(II)$ group site-specifically placed in the minor groove of right-handed DNA, the proximal deoxyriboses on opposite strands are two base pairs apart. As a consequence of the right handed helical nature of the DNA they are to the 3' side of the $EDTA \cdot Fe(II)$ group. Assuming the multiple cleavage events then result from a fixed placement followed by a diffusible reactive species such as hydroxyl radical, the average position of the $EDTA \cdot Fe(II)$ group is given by the sites of cleavage. From this position the site of the attached DNA binding unit can be determined. A model for the relationship between the cleavage pattern and the binding site for $DE \cdot Fe(II)$ is given in Fig. 10. If the major and minor orientations of $DE \cdot Fe(II)$ bind the same site, it appears the tripeptide unit of distamycin covers five base pairs. Analysis of the $ED \cdot Fe(II)$ cleavage patterns supports a similar conclusion.

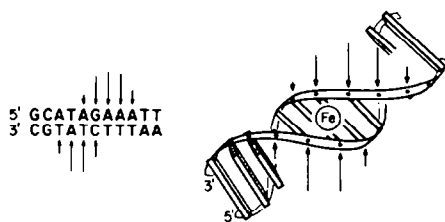


Fig. 9. Model for the asymmetric DNA cleavage patterns. Shown is the major cleavage pattern for $DE \cdot Fe(II)$ on the 381 base pair restriction fragment.

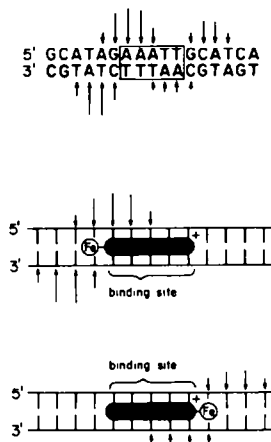


Fig. 10. Illustration relating the major DNA cleavage patterns on opposite strands to the major binding site of the tripeptide unit of $DE \cdot Fe(II)$ on the 381 base pair restriction fragment.

The carboxy terminus of the tripeptide unit is defined by the cleavage pattern produced by ED·Fe(II) and the amino terminus by the cleavage pattern produced by DE·Fe(II). The binding sites for the major and minor orientations of the tripeptide binding unit are shown in Fig. 11 for the 381 base pair fragment.

The site for the major orientation of the tripeptide unit is 3'-TTTAA-5' with the amino terminus at the 3' end of the T rich strand. The minor site is the same.

Summary. The attachment of EDTA·Fe(II) to distamycin changes the DNA binding antibiotic into a DNA cleaving molecule. The DNA cleavage patterns obtained by the sensitive Maxam-Gilbert sequencing gel methods reveal the tripeptide binding site and major orientation. EDTA-distamycin (ED), which has EDTA attached to the carboxy terminus of an N-methylpyrrole tripeptide cleaves DNA in a reaction dependent on Fe(II) and O₂ at specific A + T rich regions of heterogeneous DNA. A comparison of ED·Fe(II) and DE·Fe(II), which has EDTA attached to the amino terminus of the N-methylpyrrole tripeptide, shows similar cleavage patterns, of opposite polarity. The unequal intensity of the strand scissions of DE·Fe(II) and ED·Fe(II) cleavage allow the major binding orientation of N-methylpyrrole tripeptide, and by extension, distamycin, in the minor groove of DNA to be determined. Opposite strand analysis of the cleavage patterns for DE·Fe(II) and ED·Fe(II) allowed the position of the EDTA·Fe(II) moiety to be determined and as a result the recognition site of the tripeptide DNA binding unit. The binding site was determined to be 3'-TTTAA-5' with the amino terminus at the 3' end of the T rich strand.

This general strategy of attaching cleaving functions (in this case a chelated metal capable of redox chemistry) to DNA binding molecules, "DNA affinity cleaving", may be a useful *direct* method for determining the binding location, site size, and binding orientation of small molecules on native DNA.

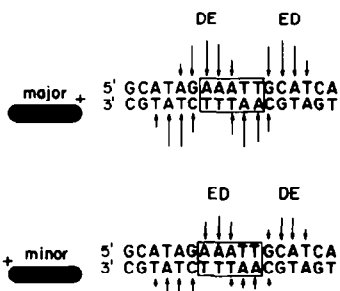


Fig. 11. Binding sites for the major and minor orientations of the tripeptide unit on the 381 base pair restriction fragment.

EXPERIMENTAL

IR spectra were recorded on a Beckman 4210 spectrophotometer. UV-visible spectra were recorded on a Beckman Model 25 spectrophotometer. ¹H NMR spectra were recorded on a Varian Associates EM-390 (90 MHz) or Bruker WM 500 (500 MHz)¹⁹ spectrometer and are reported in ppm from TMS. Mass spectra were recorded on Kratos MS-50S spectrometer equipped with a prototype SIMS ion

source (Cs⁺ ion beam).²⁰ Gel scans were performed on a Cary 219 spectrophotometer with an Apple microcomputer gel scanning program.

Flash chromatography was performed by using EM Reagents Silica Gel 60 (230-400 mesh). Reagent grade chemicals were used without purification unless otherwise stated. Dimethylformamide was dried over 4A molecular sieves. N,N'-Carbonyldimidazole was sublimed under reduced pressure prior to use. Ferrous ammonium sulfate was a Baker Analyzed Reagent. DTT was obtained from Calbiochem. Bleomycin (70% bleomycin A₂ and 30% bleomycin B₂) was generously supplied by Bristol Laboratories. MPE was prepared as previously described.⁶ All nonaqueous reactions were run under argon with rigorous exclusion of water unless otherwise noted. Doubly distilled water was used for all biological reactions and dilutions. Aqueous 5'-(α -³²P)dATP, triethylammonium salt, 3000 Ci/mmol, was from Amersham and aqueous 3'(γ -³²P)dATP, 5000-9000 Ci/mmol, was from ICN. Nucleotide triphosphates were from Boehringer Mannheim. All enzymes were from New England Biolabs except bacterial alkaline phosphatase and polynucleotide kinase which were from BRL.

Nitro acid 5. This was prepared according to the procedure of Baile¹⁴ on 10 times the described scale with the following modifications. N-Methyl-5-nitropyrrole-2-carboxylic acid was chromatographed with petroleum ether:ether (95:5) and N-methyl-4-nitropyrrole-2-carboxylic acid was eluted with petroleum ether:ether (25:75). N-Methyl-4-nitropyrrole-2-carboxyl chloride was prepared by refluxing one equivalent of N-methyl-4-nitropyrrole-2-carboxylic acid with four equivalents of thionyl chloride for 4 hr, followed by removal of excess thionyl chloride under vacuum. The acid 5 was obtained in 30% overall yield: IR (KBr) 1690, 1650, 1600, 1565, 1530, 1500, 1310, 1215, 1110 cm⁻¹; NMR (DMSO-d₆) δ 3.84 (s, 3), 3.87 (s, 3), 3.97 (s, 3), 6.85 (s, 1), 7.1 (s, 1), 7.25 (s, 1), 7.26 (s, 1), 7.45 (s, 1), 7.65 (s, 1), 8.2 (s, 1), 9.95 (s, 1), 10.35 (s, 1); UV (H₂O) 291 (35, 600), 236 nm.

EDTA-triethyl ester 9. To a soln of 10 g (0.034 mol) EDTA in 250 mL dry EtOH was added with stirring 1.5 mL H₂SO₄. The reaction was refluxed for 24 hr and the solvent was removed. Sat NaHCO₃ aq (50 ml) was added followed by 250 mL CH₂Cl₂. The layers were separated and the organic layer was washed three times with sat NaHCO₃ aq, twice with water, dried (Na₂SO₄), and concentrated to afford 11 g (80%) of crude tetraester. The ester 9 was prepared according to the procedure of Hay and Nolan.²¹ To a soln of the unpurified tetraester and 4.6 g (0.027 mol) of CuCl₂·2H₂O in 500 mL water was added with stirring 1.3 g (0.032 mol) NaOH in 7 mL water at such a rate as to maintain the pH at ca 5. The soln was then treated with H₂S and filtered. The filtrate was concentrated and purified by flash chromatography on silica gel with 10% MeOH in CH₂Cl₂ to yield 9 g (90%) of 9: IR (CH₂Cl₂) 3000, 1745, 1380, 1210 cm⁻¹; NMR (CHCl₃) δ 1.3 (t, 9 J = 9 Hz); 2.75 (s, 4), 3.3 (s, 2), 3.4 (s, 2), 3.5 (s, 4), 4.1 (q, 6, J = 7 Hz); *m/e* 376 (M⁺); TLC (silica gel, 10% MeOH in CH₂Cl₂) R_f = 0.55.

EDTA-triethylester-linker 10. To a soln of 5 g (0.013 mol) 9 and 1.52 g (0.13 mol) N-hydroxysuccinimide²² in 100 mL dioxane was added with stirring 2.7 g (0.013 mol) dicyclohexylcarbodiimide in 20 mL dioxane. The soln was stirred for 12 hr, filtered, and the filtrate concentrated. This residue was dissolved in 100 mL dimethoxyethane and added with stirring to a soln of 2 g (0.02 mol) 4-aminobutyric acid and 1.68 g (0.02 mol) NaHCO₃ in 100 mL water. After 12 hr the solvent was removed *in vacuo* and the residue purified by flash chromatography on silica gel with 10% MeOH in CH₂Cl₂ to give 4 g (65%) of 10: IR (CH₂Cl₂) 3000, 1740, 1665, 1210 cm⁻¹; NMR (DMSO-d₆) δ 1.19 (t, 9, J = 7 Hz), 1.63 (m, 2), 2.2 (t, 2, J = 6 Hz), 2.7 (t, 2, J = 6 Hz), 3.1 (m, 2), 3.19 (s, 2), 3.45 (s, 2), 3.53 (s, 4), 4.08 (m, 6), 8.0 (t, 1); *m/e* 461 (M⁺).

Nitro amine 6. To a soln of 2.5 g (6.0 mmol) 5, 0.68 g (6.6 mmol) 3-dimethylaminopropylamine, and 0.89 g

(6.6 mmol) N-hydroxybenzotriazole¹³ in 10 mL dimethylformamide (DMF) was added with stirring at 0° 1.36 g (6.6 mmol) dicyclohexylcarbodiimide. The soln was stirred at 0° for 1 hr and 25° for 12 hr. The dimethylformamide was removed under high vacuum at 35°, and the residue purified by flash chromatography on silica gel with 3% conc aqueous ammonia in MeOH to give 2.1 g (70%) of 6: IR(KBr) 3130, 2950, 1638, 1580, 1530, 1500, 1308, 1250 cm⁻¹; NMR (DMSO-d₆) δ 1.6 (m, 2), 2.15 (s, 6), 2.28 (t, 2, J = 6 Hz), 3.2 (m, 2), 3.8 (s, 3), 3.85 (s, 3), 3.95 (s, 3), 6.85 (s, 1), 7.05 (s, 1), 7.2 (s, 1), 7.27 (s, 1), 7.6 (s, 1), 8.05 (t, 1), 8.15 (s, 1), 9.95 (s, 1), 10.35 (s, 1); UV (H₂O) 286, 238 nm *m/e* 499 (M⁺).

Distamycin-EDTA-triethylester 11. A soln of 1 g (2.0 mmol) of 6 in 20 mL dimethylformamide was hydrogenated over 200 mg of 5% Pd-L at atmospheric pressure for 12 hr. The mixture was filtered through Celite affording the crude 7. To a soln of 0.93 g (2.0 mmol) 10 in 25 mL DMF was added with stirring 0.36 g (2.2 mmol) N,N'-carbonyldiimidazole in 5 mL DMF. After 2 hr, 7 was added and the resulting soln was stirred for 12 hr. DMF was removed under high vacuum at 35° and the residue purified by flash chromatography on silica gel with 3% conc aqueous ammonia in MeOH to yield 0.9 g (48%) 11: IR(KBr) 2940, 1730, 1650, 1570, 1530, 1460, 1430, 1400, 1250, 1200 cm⁻¹; NMR (DMSO-d₆) δ 1.19 (t, 9, J = 7 Hz), 1.6 (m, 2), 1.75 (m, 2), 2.13 (s, 6), 2.2 (t, 2), 2.26 (t, 2), 2.7 (m, 4), 3.1 (m, 2), 3.2 (m, 2), 3.2 (s, 2), 3.45 (s, 2), 3.55 (s, 4), 3.84 (s, 3), 3.88 (s, 3), 3.90 (s, 3), 4.08 (m, 6), 6.8 (s, 1), 6.86 (s, 1), 7.0 (s, 1), 7.16 (s, 1), 7.18 (s, 1), 7.22 (s, 1), 8.0 (t, 1), 8.05 (t, 1), 9.8 (t, 1), 9.88 (t, 1), 10.37 (s, 1); UV (H₂O) 298, 234 nm; *m/e* 912 (M⁺).

Distamycin-EDTA 3. To a soln of 0.25 g (0.37 mmol) of 11 in 5 mL EtOH was added with stirring 5 mL 0.5 M LiOH aq. The resulting soln was stirred for 12 hr and acidified to pH 4 with 10% HCl aq. The solvent was removed under vacuum at 35° and the residue purified by flash chromatography on silica gel with 20% conc aqueous ammonia in EtOH. Final purification was carried out by loading the product dissolved in water on to an Amberlite XAD-2 column and washing with 2 L water. Elution with MeOH afforded 0.15 g (66%) 3: IR(KBr): 2960, 1730, 1640, 1565, 1550, 1465, 1435, 1260, 1210, 1105 cm⁻¹; NMR (DMSO-d₆) δ 1.73 (m, 2), 1.85 (m, 2), 2.3 (t, 2, J = 7 Hz), 2.72 (s, 6), 3.05 (t, 2), 3.13 (m, 2), 3.22 (m, 2), 3.4 (t, 2, J = 6 Hz), 3.45 (t, 2, J = 6 Hz), 3.8 (s, 3), 3.82 (s, 3), 3.83 (s, 3), 3.93 (s, 4), 4.04 (s, 2), 4.17 (s, 2), 6.91 (s, 1), 6.93 (s, 1), 7.05 (s, 1), 7.18 (s, 1), 7.22 (s, 1), 7.26 (s, 1), 8.25 (t, 1), 8.86 (t, 1), 9.95 (s, 1), 9.97 (s, 1), 10.15 (s, 1); UV (H₂O): 297 (35,600), 236 nm (29,400); *m/e* 866 (C₇H₅₃N₁₁O₁₁K⁺).

Nitro amine 12. To a soln of 2.5 g (6.0 mmol) of 5 in 50 mL DMF was added with stirring 1.07 g (6.6 mmol) N,N'-carbonyldiimidazole¹⁵ in 10 mL DMF. After 2 hr, 9.6 g (66 mmol) 3,3'-diamino-N-methyl-dipropylamine was quickly added and the resulting soln was stirred for 12 hr. The DMF was removed under high vacuum at 35° and the residue was triturated three times with ether. The crude product was purified by flash chromatography on silica gel with 12% conc aqueous ammonia in MeOH to yield 2.3 g (68%) of 12: IR(KBr) 2960, 1640, 1580, 1530, 1311, 1210 cm⁻¹; NMR (DMSO-d₆) δ 1.46 (m, 2), 1.6 (m, 2), 2.12 (s, 3), 2.33 (t, 4, J = 7 Hz), 2.55 (s, 2), 3.2 (m, 4), 3.80 (s, 3), 3.86 (s, 3), 3.96 (s, 3), 6.8 (s, 1), 7.04 (s, 1), 7.2 (s, 1), 7.27 (s, 1), 7.6 (s, 1), 8.05 (t, 1), 8.2 (s, 1), 9.94 (s, 1), 10.3 (s, 1); UV (H₂O) 294, 239 nm; *m/e* 542 (M⁺).

Nitro EDTA-triethylester 13. To a soln of 1.39 g (3.7 mmol) of 9 in 25 mL DMF was added with stirring 0.66 g (4.07 mmol) N,N'-carbonyldiimidazole¹⁵ in 5 mL DMF. After 2 hr, 2 g (3.7 mmol) of 12 was added and the resulting soln was stirred for 12 hr. DMF was removed under high vacuum at 35° and the residue was purified by flash chromatography on silica gel with 3% conc aqueous ammonia in EtOH to yield 2.5 g (75%) of 13: IR(KBr) 2950, 1735, 1640, 1590, 1525, 1500, 1438, 1400, 1310, 1255, 1210; NMR (DMSO-d₆) δ 1.15 (t, 9, J = 7 Hz), 1.55 (m, 2), 1.6 (m,

2), 2.12 (s, 3), 2.7 (m, 4), 3.12 (m, 2), 3.18 (s, 2), 3.20 (m, 2), 3.44 (s, 2), 3.5 (s, 4), 3.8 (s, 3), 3.86 (s, 3), 3.97 (s, 3), 4.05 (m, 6), 6.82 (s, 1), 7.05 (s, 1), 7.19 (s, 1), 7.27 (s, 1), 7.59 (s, 1), 7.96 (t, 1), 8.03 (t, 1), 8.18 (s, 1), 8.56 (s, 1), 8.9 (s, 1); UV (H₂O) 288, 240 nm; *m/e* 900 (M⁺).

EDTA-distamycin-triethylester 14. A soln of 1 g (1.11 mmol) of 13 in 10 mL DMF was hydrogenated over 200 mg of 5% Pd-C at atmospheric pressure for 12 hr. The mixture was filtered through Celite affording the crude 15. To a soln of 0.08 g (1.33 mmol) AcOH in 3 mL DMF was added with stirring 0.22 g (1.33 mmol) N,N'-carbonyldiimidazole in 3 mL DMF. After 2 hr, 15 was added and the resulting soln was stirred for 12 hr. DMF was removed under high vacuum at 35° and the residue purified by flash chromatography on silica gel with 2% conc aqueous ammonia in MeOH to yield 0.55 g (54%) of 14: IR(KBr) 2950, 1730, 1650, 1580, 1550, 1535, 1460, 1440, 1400, 1260, 1210 cm⁻¹; NMR (DMSO-d₆) δ 1.17 (t, 9, J = 7 Hz), 1.55 (m, 2), 1.6 (m, 2), 1.97 (s, 3), 2.12 (s, 3), 2.28 (m, 4), 2.65 (m, 2), 2.70 (m, 2), 3.12 (m, 2), 3.17 (s, 2), 3.17 (m, 2), 3.44 (s, 2), 3.5 (s, 4), 3.85 (s, 3), 3.88 (s, 3), 3.9 (s, 3), 4.08 (g, 6, J = 7 Hz), 6.8 (s, 1), 6.84 (s, 1), 6.98 (s, 1), 7.02 (s, 1), 7.14 (s, 1), 7.17 (s, 1), 7.22 (s, 1), 7.62 (s, 1), 7.97 (t, 1), 8.02 (t, 1), 9.83 (s, 1), 9.9 (s, 1); UV (H₂O) 304, 235 nm; *m/e* 912 (M⁺).

EDTA-distamycin 4. To a soln of 0.25 g (0.27 mmol) of 14 in 5 mL EtOH was added with stirring 5 mL 0.5 M LiOH aq. The resulting soln was stirred for 12 hr and acidified to pH 4 with 10% HCl aq. The solvent was removed under high vacuum at 35° and the residue purified by flash chromatography on silica gel with 3% conc ammonia in MeOH to yield 0.17 g (75%) of the ammonium salt of ED 4: IR (KBr) 2950, 1635, 1580, 1460, 1430, 1400, 1255, 1205, 1105 cm⁻¹; NMR (D₂O) δ 1.87 (s, 3), 1.9 (m, 4), 2.8 (s, 3), 2.9–3.13 (m, 12), 3.17–3.3 (m, 6), 3.53 (s, 3), 3.57 (s, 3), 3.6 (s, 3), 3.67 (s, 2), 6.42 (s, 1), 6.48 (s, 1), 6.56 (s, 1), 6.8 (s, 1), 6.83 (s, 1), 6.87 (s, 1); UV (H₂O) 303 nm (35,000 est.) 235 (29,500 est.); *m/e* 828 (M⁺).

Preparation of supercoiled pBR322 DNA and end-labeled restriction fragments. DNA for this investigation was bacterial plasmid pBR322 whose entire sequence is known.²³ The plasmid was grown in *E. coli* strain HB101 and isolated by the methods of Tanaka and Weissblum.²⁴ Superhelical pBR322 plasmids, containing 98.5% form I DNA, were first digested with the restriction endonuclease EcoRI and then labeled at the 3' end with [α-³²P]dATP and the Klenow fragment of DNA polymerase I.¹⁸ A second enzymatic digest with the restriction endonuclease Rsa I yielded two end labeled fragments, 167 and 516 nucleotides in lengths. These were isolated by gel electrophoresis on a 5% polyacrylamide, 1:30 crosslinked, 2 mm thick gel. Isolation of the two fragments from the gel and subsequent procedures were similar to those of Maxam-Gilbert.¹⁷ In a similar fashion, pBR322 DNA was restricted with Bam HI and labeled at the 3' end. Further restriction with Eco RI and Sal I yielded a 381 and a 279 base pair fragment respectively. The 381 base pair fragment was 5' labeled at the Bam HI site by cleavage of pBR322 with Bam HI, treatment with bacterial alkaline phosphatase, followed by treatment with (γ³²P)-ATP and polynucleotide kinase.¹⁷ Further restriction with Eco RI yielded the desired fragment.

Cleavage reactions. All reactions were run with freshly prepared drug-iron complexes. Equimolar drug-Fe(II) complexes were made by combining aqueous drug stock solutions (~10 mM, checked spectrophotometrically before use) with a 10 mM aqueous ferrous ammonium sulfate solution and then diluting with water to the appropriate drug-iron concentration. The cleavage reactions were initiated by adding 2 μl of a drug-Fe(II) solution to 16 μl of a buffered DNA solution (final concentrations and buffers and in figure legends) followed by 2 μl of an aqueous 10 mM DTT solution. The reactions were thoroughly mixed by vortexing, spun down and incubated at 25° for 30 min.

Analysis of the cleavage efficiency. The cleavage reactions

were conducted with 10 μ M pBR322 superhelical DNA containing >98% from I DNA. After 1/2 hr at 25° the reactions were quenched with 4 μ l of a 50 mM disodium EDTA, 10% ficol soln and electrophoresed on a 1% agarose gel at 120 V for 4 hr. The gel was then stained with ethidium bromide, destained and photographed with polaroid type 55 positive-negative land film under long wavelength UV irradiation. The negative film was then scanned at 485 nm on a Cary 219 spectrophotometer and the peak areas of the form I, II and III bands were determined by a gel scanning program. The data was then corrected for the decreased stainability of form I DNA,⁶ and for the presence of 1.5% form II in the original sample.

Analysis of the sequence specificity of the cleavage reactions. The cleavage reactions were run with >600 cpm of ³²P 3' end labeled restriction fragments made up to a total DNA concentration of 100 μ M (bp) with sonicated calf thymus DNA. The reactions were run at 25° for 1/2 hr and terminated by lyophilization and suspension in 4 μ l of a pH 8.3 100 mM Tris-Borate, 50% formamide soln. These were then loaded on a 0.4 mm thick, 40 cm long, 8% polyacrylamide, 1:20 crosslinked, 50% urea gel and electrophoresed at 1500 V until xylene cyanol tracking dye was at the bottom of the gel. Autoradiography of the gels was carried out at -50° on Kodak, X-Omat AR film and the autoradiograms were then scanned at 485 nm. The relative peak area for a particular site was equated to the relative cleavage efficiency.

REFERENCES

- ¹Supported by Fellowship DRG-526 of the Damon Runyon-Walter Winchell Cancer Fund.
²IBM Fellow 1982-83.
³Camille and Henry Dreyfus Teacher Scholar, 1978-83.
⁴*Bleomycin: Chemical Biochemical and Biological Aspects* (Edited by S. M. Hecht). Springer-Verlag, New York (1979); R. M. Burger, J. Peisach, S. B. Horowitz, *Life Sci.* **28**, 715 (1981).
⁵M. Takeshita, L. Kappen, A. P. Grollman, M. Eisenberg and I. Goldberg, *Biochemistry* **20**, 7599-7606 (1981); M. Takeshita, A. P. Grollman, E. Ohtusbo and H. Ohtsubo, *Proc. Natl Acad. Sci. USA*, **75**, 5983 (1978). A. D. D'Andrea and W. A. Haseltine, *Ibid.* **75**, 3608 (1978).
⁶R. P. Hertzberg and P. B. Dervan, *J. Am. Chem. Soc.* **104**, 313 (1982).
⁷M. J. Waring, *J. Mol. Biol.* **13**, 269 (1965); J.-B. LePecq and C. Paoletti, *J. Mol. Biol.* **27**, 87 (1967); ^bW. Muller and D. M. Crothers, *Eur. J. Biochim.* **54**, 267 (1975); ^cJ. L. Bresloff and D. M. Crothers, *Biochemistry* **20**, 3457 (1981). See also ^dR. V. Kastrup, M. A. Young and T. R. Krugh, *Ibid.* **17**, 4885 (1978).
⁸For a description of "MPE · Fe(II) footprinting" see ^aM. W. Van Dyke, R. P. Hertzberg and P. B. Dervan, *Proc. Nat. Acad. Sci. USA* **79**, 5470 (1982); ^bM. W. Van Dyke and P. B. Dervan, *Symposia on Quantitative Biology* **47**, Cold Spring Harbor **47**, 347 (1983); ^cM. W. Van Dyke and P. B. Dervan, *Biochemistry* **22**, 2373 (1983).
⁹K. E. Reinert, *J. Mol. Biol.* **72**, 592 (1972). ^bG. Luck, Ch. Zimmer, K. E. Reinert and F. Arcamore, *Nucl. Acids Res.* **4**, 2655 (1977); ^cB. Nosikov and B. Jain, *Ibid.* **4**, 2263 (1977); ^dFor reviews see: Ch. Zimmer, *Progress in Nucleic Acids Research and Molecular Biology* (Edited by N. E. Cohn) Vol. XV, p. 285. Academic Press, New York (1975). ^eE. F. Gale *et al.*, *The Molecular Basis of Antibiotic Action*, p. 345. Wiley-Interscience, New York (1981).
¹⁰G. Luck, M. Treibel, M. Waring and Ch. Zimmer, *Nucl. Acids Res.* **1**, 5039 (1974); ^aA. S. Zasedatelev, A. L. Zhuze, Ch. Zimmer, S. L. Grokhovsky, V. G. Tumanyan, G. V. Gursky and B. P. Gottikh, *Dokl. Acad. Nauk. SSSR* **231**, 1006 (1976); ^cA. S. Krylov, S. L. Grokhovsky, A. S. Zasedatelev, A. L. Zhuze, G. V. Gursky and B. P. Gottikh, *Nucl. Acids Res.* **6**, 289 (1979).
¹¹H. M. Berman, S. Neidle, Ch. Zimmer and H. Thrum, *Biochim. Biophys. Acta.* **561**, 124 (1979); ^bL. A. Marky, K. S. Blumenfeld and K. G. Breslouer, *Nucleic Acids Res.* **11**, 2857 (1983).
¹²P. G. Schultz, J. S. Taylor and P. B. Dervan, *J. Am. Chem. Soc.* **104**, 6861 (1982).
¹³W. Koenig and R. Geiger, *Chem. Ber.* **103**, 788 (1970).
¹⁴M. Bialer, B. Yagen and R. Mechoulam, *Tetrahedron* **34**, 2389 (1978).
¹⁵R. Paul and G. W. Anebrison, *J. Org. Chem.* **27**, 2094 (1962).
¹⁶J. E. Strong, S. T. Crooke, *Bleomycin: Chemical, Biochemical and Biological Aspects* (Edited by S. M. Hecht) p. 244. Springer-Verlag, New York (1979); ^bP. H. Johnson and L. I. Grossman, *Biochemistry* **16**, 4217 (1977).
¹⁷A. M. Maxam and W. Gilbert, *Methods Enzymol.* **65**, 499 (1980).
¹⁸F. Sanger and A. R. Coulson, *J. Mol. Biol.* **94**, 441 (1980).
¹⁹We gratefully acknowledge the Southern California Regional NMR Facility (NSF grant 7916324A1).
²⁰We gratefully acknowledge the Bio-organic, Biomedical Mass Spectrometry Resource (A. L. Burlingame, Director) at UC, San Francisco supported by NIH Research Grant No. RR00719 from the Division of Resources and the Middle Atlantic Mass Spectrometry Laboratory (R. Cotter, Director) at Johns Hopkins University.
²¹R. W. Hay and K. B. Nolan, *J. Chem. Soc. Dalton* 1348 (1975).
²²G. W. Anderson, J. E. Zimmerman and F. M. Callahan, *J. Am. Chem. Soc.* **86**, 1839 (1964).
²³J. G. Sutcliffe, *Cold Spring Harbor Symp. Quant. Biol.* **43**, 77 (1979).
²⁴Preparation of: T. Tanaka and B. Weisblum, *J. Bacteriol.* **121**, 354 (1974).